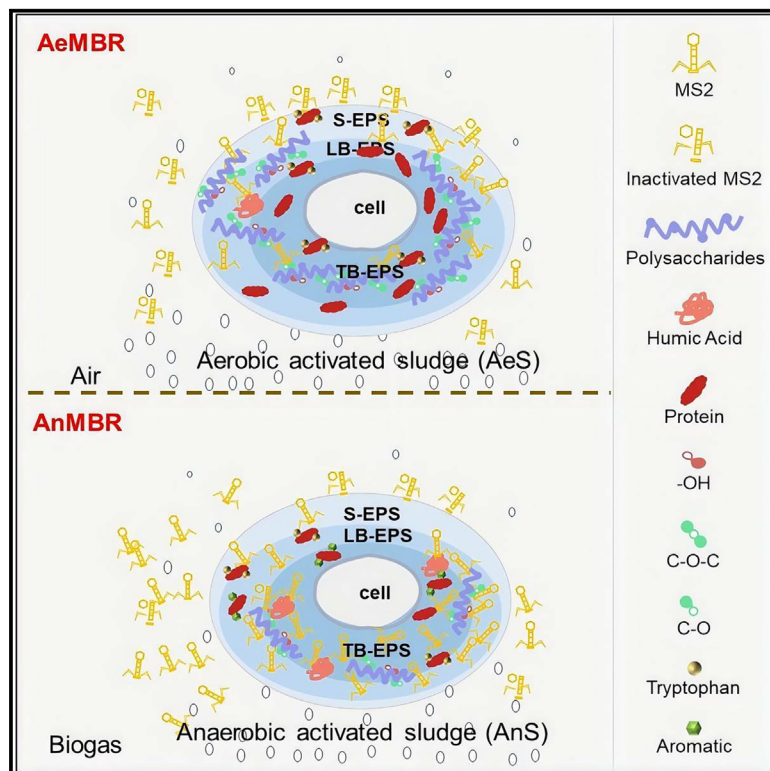


Comparison of activated sludge and virus interactions in aerobic and anaerobic membrane bioreactors

Graphical abstract



Authors

Jinfan Zhang, Jie Zhang, Daisuke Sano, Rong Chen

Correspondence

chenrong@xauat.edu.cn

In brief

Applied microbiology; Biological waste treatment; Water resources engineering

Highlights

- The average virus removal efficiency of AeMBR was higher than that of AnMBR
- S-EPS was the primary contributor to virus adsorption in AeS
- TB-EPS played a significant role in virus adsorption in AnS
- Virus inactivation in aerobic mixed liquor exceeded that in the anaerobic mixed liquor



Article

Comparison of activated sludge and virus interactions in aerobic and anaerobic membrane bioreactors

Jinfan Zhang,¹ Jie Zhang,¹ Daisuke Sano,^{2,3} and Rong Chen^{1,4,5,*}¹Shaanxi Key Laboratory of Environmental Engineering, School of Environmental and Municipal Engineering, Xi'an University Architecture and Technology, No. 13 Yanta Road, Xi'an 710055, P.R. China²Department of Civil and Environment Engineering, Graduate School of Engineering, Tohoku University, Aoba 606-06, Aramaki, Aoba-ku, Sendai, Miyagi 980-8579, Japan³Department of Frontier Sciences for Advanced Environment, Graduate School of Engineering, Tohoku University, Aoba 6-6-06, Aramaki, Aoba-ku, Sendai, Miyagi 980-8579, Japan⁴International S&T Cooperation Center for Urban Alternative Water Resources Development, Key Laboratory of Northwest Water Resource, Environment and Ecology, MOE, Xi'an University of Architecture and Technology, No. 13 Yanta Road, Xi'an 710055, P.R. China⁵Lead contact*Correspondence: chenrong@xauat.edu.cn<https://doi.org/10.1016/j.isci.2024.111450>

SUMMARY

Membrane bioreactors (MBRs) are effective sewage treatment technologies, yet the differences in virus removal efficiency between aerobic (AeMBR) and anaerobic membrane bioreactors (AnMBR), remain inadequately understood. This study compared the virus removal efficiency of AeMBR and AnMBR, focusing on the interactions between aerobic (AeS) and anaerobic (AnS) activated sludge and viruses in the sewage treatment process. Results showed average log removal values (LRVs) for MS2 of 2.53 ± 0.54 in AeMBR and 1.64 ± 0.90 in AnMBR due to the higher virus inactivation in the aerobic mixed liquor. The virus concentration in AnS was greater than in AeS, consistent with the predictions from the pseudo-second-order kinetic model. Soluble extracellular polymeric substances (S-EPS) were key to virus adsorption in AeS, while tightly bound EPS (TB-EPS) were significant in AnS. Additionally, more fluorescent substances in AnS contributed to virus adsorption, while more functional groups in AeS offered adsorption sites.

INTRODUCTION

The membrane bioreactors (MBRs) are an advanced sewage treatment process that combines membrane separation with biological processes, offering advantages such as small footprints and high-quality effluent.¹ MBRs are divided into aerobic MBR (AeMBR) and anaerobic MBR (AnMBR) based on biological processes. AeMBR utilizes microorganisms to metabolize and degrade organic matter under aerobic conditions, effectively achieving the removal of organic pollutants. In contrast, AnMBR converts organic matter into bioenergy through anaerobic digestion, producing nutrient-rich effluent suitable for agricultural use.² While AeMBR has been widely adopted in sewage treatment, AnMBR is often regarded as impractical for similar applications due to concerns about achieving comparable transmembrane flux rates. Nonetheless, the AnMBR is gaining recognition as a viable alternative treatment technology for sewage, owing to its potential for energy generation and low sludge production.

As the population grows and urbanization accelerates, water demand continues to rise, leading to a significant increase in sewage reuse. However, concern regarding the public health

risk associated with exposure to viruses present in sewage is critical limiting to the widespread adoption of sewage reuse.^{3,4} To address these concerns, the virus removal efficiency in MBRs has been well studied.^{5–7} The log removal value (LRV) of human pathogenic viruses in actual sewage using lab-scale AnMBR ranged from 2.31 to 5.0, whereas the average LRV of viruses in full-scale AeMBR was between 3.9 and 7.1.^{6,7} In the MBR treatment of sewage, viruses are adsorbed by activated sludge (AS) within the bioreactor and subsequently trapped by the membrane. The trapped viruses are inactivated through predation or enzymatic breakdown. Therefore, the interaction between AS and virus is crucial to the removal efficiency of MBRs.^{5,7} A key factor influencing the interactions between AS and virus is the presence of extracellular polymeric substances (EPS), which determine the surface properties of AS and significantly affect interactions through functional groups and hydrophobic interactions.^{8,9} Additionally, EPS contributes to virus inactivation due to abundant redox-active components.¹⁰ EPS are categorized into soluble EPS (S-EPS) and bound EPS (B-EPS), with the latter further classified into tightly bound (TB-EPS) inner layer and loosely bound EPS (LB-EPS) outer layer based on structure, while carbohydrates and proteins typically



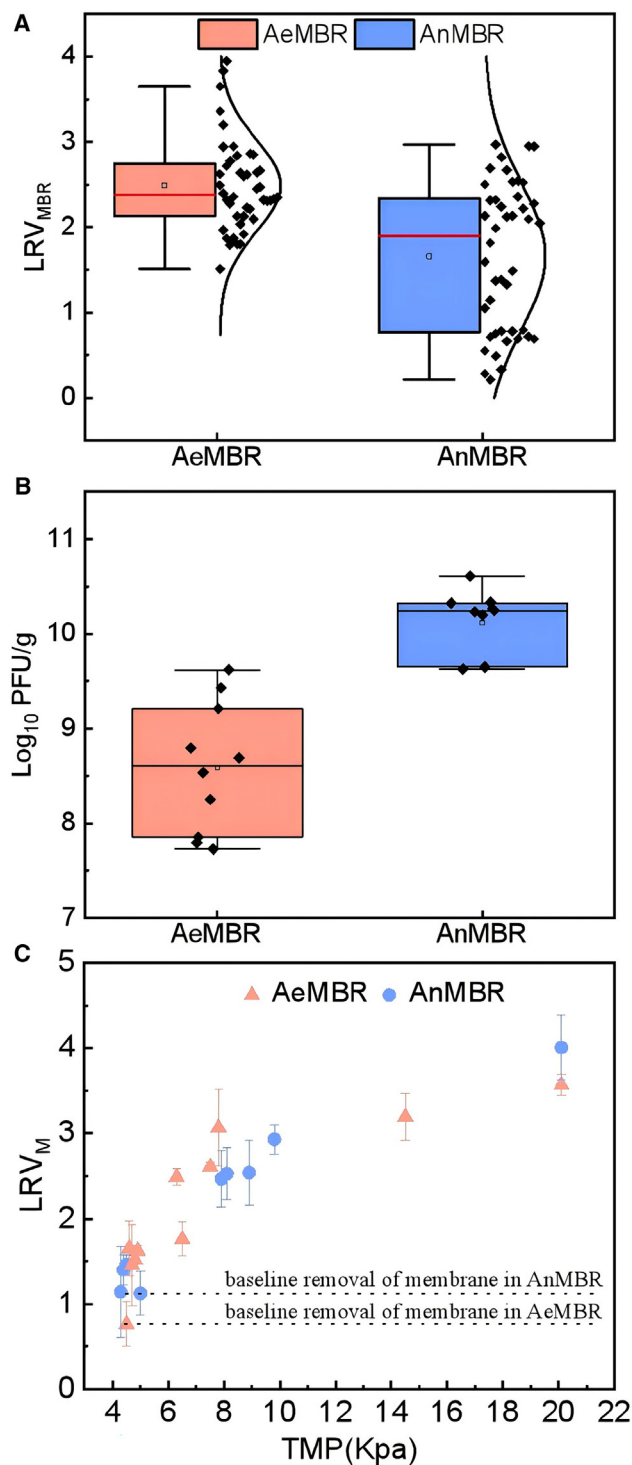


Figure 1. Virus removal performance of AnMBR and AeMBR
(A) Virus removal efficiency in AnMBR and AeMBR, respectively.
(B) MS2 adsorption amount weighed by MLSS mass in activated sludge.
(C) Virus rejection by membrane and membrane fouling.

constitute the predominant components of EPS, accounting for approximately 20% of the total content.¹¹

Although both AeMBR and AnMBR integrate the bioreactors with the membrane modules, they differ in several key aspects, including physiochemical environments, microbial niches, metabolic products, and characteristics of membrane fouling.^{1,12} Specifically, EPS in AeMBR are typically rich in proteins and polysaccharides linked to aerobic microbial metabolism, whereas AnMBR tends to contain a higher proportion of humic substances and polysaccharides. Additionally, the EPS yield in AeMBR is generally greater than that in AnMBR due to the heightened activity of aerobic microorganisms. Furthermore, the particle size of anaerobic activated sludge (AnS) is usually an order of magnitude smaller than that of aerobic activated sludge (AeS). These differences contribute to variations in virus adsorption and inactivation by AS in AeMBR and AnMBR, resulting in differing virus removal efficiencies in the two types of MBRs and consequently presenting varying levels of public health risks.^{8,9} Another critical factor is that the aerobic conditions in AeMBR enhance virus inactivation within the mixed liquor.^{13,14}

Despite advancements in the investigation of virus removal efficacy in AeMBR and AnMBR, a comprehensive comparison of both MBRs of respective efficiencies and characteristics in virus removal remains elusive due to the confounding effects of sewage characteristics and operational parameters. This research gap hinders our understanding of optimizing MBR systems, particularly in enhancing the virus removal efficiency from sewage. Consequently, this study employed MS2 as a surrogate virus to compare the efficacy of virus removal in AeMBR and AnMBR during sewage treatment, focusing on the adsorption and inactivation between AS and virus, thereby providing novel insights for the advancement of MBR technologies in sewage treatment.

RESULTS AND DISCUSSION

Virus removal performance of membrane bioreactors

The AeMBR and AnMBR achieved average COD removal efficiencies of $94.88\% \pm 2.43\%$ and $90\% \pm 1.71\%$, respectively (Figure S1A). The COD conversion to CH₄ in AnMBR was 74.9% with CH₄ content of $88.2 \pm 1.3\%$ (Figure S1B). The MLVSS/MLSS ratios of AeMBR and AnMBR were consistently 0.81 ± 0.05 and 0.93 ± 0.02 , respectively, indicating the high biomass and biological activity in mixed liquor of both MBRs (Figure S1C).¹⁵ The stable biological performance and consistent COD removal efficiency demonstrated the performance stability of MBRs during operation.

The average LRV for MS2 of the AeMBR and AnMBR were 2.53 ± 0.54 and 1.64 ± 0.90 , respectively, indicating significant variability in MS2 removal, particularly in AnMBR (Figure 1A). The virus concentrations in AeS and AnS of the MBRs were $9.72 \log_{10}$ PFU/g, and $10.89 \log_{10}$ PFU/g, respectively, indicating the high virus adsorption of AS in MBRs (Figure 2B). Similarly, AS in anaerobic-anoxic-oxic (A2O) processes also demonstrated strong virus adsorption capabilities.^{16,17} However, research on virus adsorption by wastewater solids suggests that wastewater solids have a limited virus adsorption capacity.¹⁸ The comparison between the virus adsorption of AS and wastewater solids

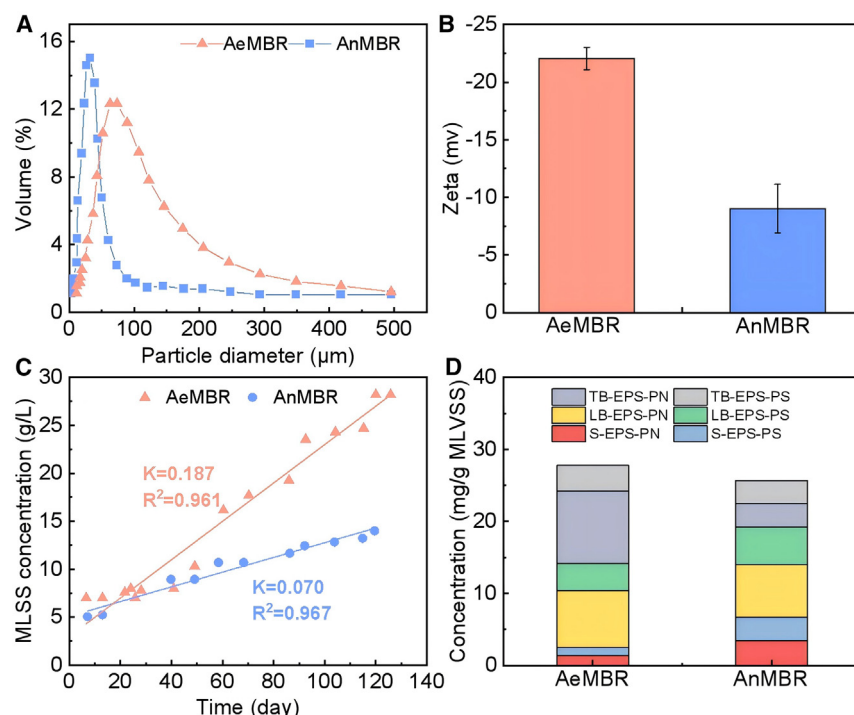


Figure 2. Properties of activated sludge associating virus adsorption

(A) The particle size distribution.
(B) Zeta potential.
(C) Activated sludge growth rate.
(D) The production of EPS (PN, protein; PS, polysaccharide).

to 248.90 μm with a mean value of 31.50 μm (Figure 2A). Previous studies on the distribution of viruses in MBRs have demonstrated that smaller particle sizes are associated with greater virus adsorption.^{5,6} The higher proportion of smaller particle sizes in AnS resulted in increased virus adsorption. Electrostatic interactions between virus and solid surface are generally considered to govern adsorption characteristics, followed by hydrophobic interactions, van der Waals forces, and others.^{9,21} Electrostatic repulsion between viruses and like-charged solid surfaces hinders or completely inhibits adsorption. The average zeta potential of AeS and AnS was -22.06 ± 0.86 mV and

highlights the significance of microorganisms and metabolic metabolites in the virus adsorption process. Furthermore, the differences in virus concentrations in AS from AeMBR, AnMBR, and the A2O process suggest that the types of microorganisms and metabolites significantly influence virus adsorption in AS. The contribution of membrane alone to LRV in AeMBR and AnMBR referred to as the “baseline removal,” was 0.76 and 1.12, respectively. As membrane fouling accumulated, the virus removal efficiency of membrane fouling in MBRs improved, with the impact of membrane fouling on virus removal being more pronounced in AnMBR compared to AeMBR (Figure 1C). Overall, the LRV of AeMBR was higher than AnMBR, while viral adsorption was significantly higher of the AnS compared to AeS in MBRs, and membrane fouling improved the virus retention efficiency.

Generally, three mechanisms are related to virus removal in the MBRs: (i) virus adsorption to activated sludge, (ii) virus inactivation within mixed liquor, and (iii) virus retention by membrane and membrane fouling.⁷ By adjusting process conditions, operating parameters, and exogenous additives, the characteristics of activated sludge and membrane fouling process can be regulated, thereby enhancing virus removal efficiency.¹⁹ Wang et al. demonstrated an improved method for virus removal integrating electrochemical with MBR technology.²⁰ Additionally, the virus removal efficiency of AnMBR was enhanced by regulating the particle size distribution of mixed liquor and the composition of membrane fouling.^{5,6}

Properties of activated sludge associated with virus adsorption

The particle size of AeS ranged from 13.01 μm to 497.83 μm with a mean value of 85.2 μm , and AnS varied from 7.78 μm

-8.96 ± 2.1 mV, respectively, indicating that the electrostatic repulsion between MS2 and AeS was significantly greater than that between MS2 and AnS, attributed to the net negative charge of MS2 in the mixed liquor (Figure 2B). The disparity in electrostatic repulsion between the virus and AS suggests that the adsorption efficiency of the virus by AnS was superior to that of AeS. Figure 2C illustrates that the growth rate for AeS was 0.18 g/(L·d), and AnS was 0.07 g/(L·d), excluding the effects of endogenous digestion. The additional virus adsorption attributed to the growth of AS was calculated to be 8.15 log₁₀ PFU/d for AeS and 9.26 log₁₀ PFU/d for AnS based on growth rate and MS2 concentration in AS. Throughout the entire run, the total quantity of virus from AeMBR and AnMBR entering the environment through AS discharge was 10.71 log₁₀ PFU and 11.11 log₁₀ PFU, respectively (Figure S2). AS from MBRs is believed to be a reservoir with abundant virus, implying the exposure and transmission risk during AS treatment and disposal, particularly for AnS. In terms of the specific production of EPS expressed by protein and carbohydrate production per gram MLVSS, the concentration of total protein and polysaccharide in the AS from the AeMBR and AnMBR were 27.79 mg/g MLVSS and 25.62 mg/g MLVSS, respectively (Figure 2D). The differences in virus adsorption characteristics between AeS and AnS could be influenced by the total amount and composition of EPS.

Adsorption behavior of activated sludge to virus

In order to better understand the interactions between viruses and AS, the pseudo-second-order kinetic model was employed to describe the adsorption behavior of viruses at AS concentrations of 6 g/L, 8 g/L, and 10 g/L, with fitting coefficients indicating that the adsorption processes of both AeS and AnS to the virus

Table 1. Constants and fitting coefficients of pseudo-second-order kinetic model

Parameter	6 g/L	8 g/L	10 g/L
AeS			
q_e (PFU/g)	$11.40 \log_{10}$	$11.36 \log_{10}$	$11.13 \log_{10}$
K_2 (g/(PFU·min))	$8.03 \times 10^{(-13)}$	$9.68 \times 10^{(-12)}$	$3.06 \times 10^{(-11)}$
R^2	0.9192	0.9987	0.9981
AnS			
q_e (PUF/g)	$11.52 \log_{10}$	$11.93 \log_{10}$	$11.91 \log_{10}$
K_2 (g/(PFU·min))	$4.57 \times 10^{(-12)}$	$3.46 \times 10^{(-12)}$	$7.07 \times 10^{(-11)}$
R^2	0.9991	0.9978	0.9997

can be effectively described by this model (Figure S3; Table 1). The adsorption equilibrium time was between time and MS2 adsorption efficiency prior to assessing the adsorption capacity of AS at varying concentrations (Figure S4). The results indicated that the rate-limiting steps of both AeS and AnS were chemisorption processes, consistent with findings from Wei et al.²² In a range of 6 g/L to 10 g/L, there was little difference in the predicted q_e values for AeS and AnS, suggesting that MLSS concentration may not be a key operational parameter for improving virus removal in MBRs. The predicted q_e values for AnS were higher than those for AeS within the MLSS concentration range of 6 g/L to 10 g/L, indicating that AnS has a greater virus adsorption capacity. The MS2 concentration on AeS of AeMBR ($9.72 \log_{10}$ PFU/g) was lower than the predicted q_e values ($11.13 \log_{10}$ PFU/g), while the predicted q_e value ($11.91 \log_{10}$ PFU/g) closely matched the MS2 concentration on AnS in AnMBR ($10.89 \log_{10}$ PFU/g). We speculated that the longer SRT in AnMBR facilitates the saturation of viral adsorption on AS, contributing to its higher adsorption concentration.

Survivability of infective virus surrogate

The MS2 inactivation rates in aerobic mixed liquor were higher than those in the anaerobic mixed liquor, probably owing to the DO and differing compositions of microorganisms (Figure 3A). However, the virus inactivation rate in inactivated AeS was lower than that in inactivated AnS, indicating that the activity of aerobic microorganisms has a more pronounced effect on virus inactivation compared to anaerobic microorganisms (Figure 3A). Previous studies have confirmed that DO contributes to the loss of viral infectivity through the oxidative destruction of viral capsid proteins, making it a key factor in virus inactivation in sewage.^{13,14} Moreover, the introduction of biological factors, especially microorganisms, alters the virus inactivation in mixed liquor.^{18,23} The redox reaction between microorganisms and microbial metabolites in the aerobic mixed liquor is more prone to occur, thereby enhancing virus inactivation.¹⁰ The virus inactivation rate in aerobic mixed liquor surpassed that in the anaerobic mixed liquor, potentially contributing significantly to the higher virus removal efficiency observed in the AeMBR compared to the AnMBR.

The virus inactivation rate constants were 0.41 days^{-1} , 1.44 days^{-1} , and 0.45 days^{-1} in aerobic mixed liquor, at the DO concentration of 0 mg/L, 2 mg/L, and 4 mg/L, respectively (Figure 3B). The virus inactivation rate did not rise with the in-

crease in DO concentration, with the highest inactivation rate constant observed at a DO concentration of 2 mg/L. The aerobic mixed liquor was obtained from the acclimatized activated sludge with 2 mg/L of DO concentration, indicating that the virus inactivation at a DO concentration of 2 mg/L may be largely attributed to higher microbial activity in the survivability experiment.

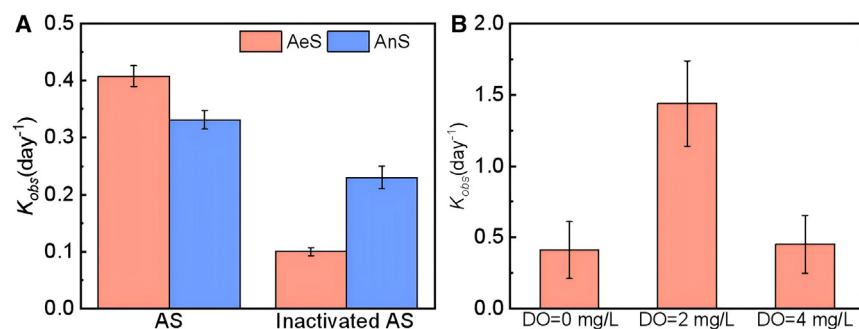
The virus is also inactivated by the physical action of the air-water interface (AWI) produced by the aeration of MBRs.²⁴ At the same aeration intensity, the smaller particle size of AnS generates more AWI than AeS, a factor that was overlooked in the batch experiment.^{25,26} Although MS2 is commonly used as a surrogate virus for human enteroviruses in virus studies, it is important to note that MS2, as a typical non-enveloped virus, differs significantly from enveloped viruses due to fragile lipid envelop.⁸ Consequently, the conclusions drawn regarding the inactivation of MS2 in aerobic and anaerobic mixed liquor may not be applicable to enveloped viruses.

Interactions between activated sludge and virus Adsorption kinetic changes

The pseudo-second-order kinetic model was employed to fit the adsorption capacity of each AS fraction at equilibrium, thereby assessing the contribution of each fraction to virus adsorption. Under a MS2 concentration of 10^{10} PFU/L and 25°C , the adsorption kinetics of S-EPS, LB-EPS, and TB-EPS were investigated following the extraction of AS to explore the interactions between each EPS fraction and the virus (Figure S5; Figure S6; Table 2). The pseudo-second-order kinetic model effectively characterizes the adsorption behavior of S-EPS and LB-EPS, but not TB-EPS. The q_e value after the S-EPS extraction of AeS was one order of magnitude lower than that of untreated AeS, highlighting the significant role of S-EPS in virus adsorption within AeS. While the maximum adsorption capacity after the TB-EPS extraction of AnS was not determined, the q_e values of AnS after the S-EPS and LB-EPS extraction were comparable to the predicted q_e value of untreated AnS, suggesting the predominant role of TB-EPS in virus adsorption by AnS.

Spectra changes

The peaks of S-EPS in AeS were observed at excitation/emission wavelengths (Ex/Em) of approximately 276/335 nm, 336/420 nm, and 250/375 nm, corresponding to tryptophan protein-like substances, humic acid-like substances and humic acid, respectively. The peaks of LB-EPS and TB-EPS of AeS were detected at Ex/Em around 305/375 nm, identified as human acid (Figure S7). The peak of EPS in AnS was found at Ex/Em of about 230/330 nm and 276/335 nm, representing tyrosine aromatic protein-like substances and tryptophan protein-like substances, respectively (Figure S8). Further, the changes in the content and composition of EPS fractions before and after virus adsorption were analyzed using three-dimensional fluorescence spectra combined with parallel factor analysis (PARAFAC), as illustrated in Figure S9. Table 3 summarizes the variations in fluorescence intensity of EPS fractions before and after MS2 adsorption. The fluorescence intensity of tryptophan protein-like substance in S-EPS of AeS decreased from 205 to 103. Similarly, the fluorescence intensities of marine humic acid and tryptophan protein-like substances in B-EPS of AeS decreased from 1312 to

**Figure 3. Virus inactivation in mixed liquor**

(A) virus inactivation in AeS and AnS, respectively. (B) Virus inactivation rate constants in different DO concentrations.

1198 and from 1956 to 1736, respectively. The decrease in fluorescence intensity indicates that these substances of AeS were bound to MS2, as evidenced by fluorescence quenching.²⁷ Different from AeS, the tyrosine aromatic protein-like substance, tryptophan protein-like substance, humic acid A, and humic acid B in the EPS of AnS bound to viruses. Notable differences in virus-binding fluorescence substances were observed between different AS and EPS fractions were seen. Additionally, the protein-like substance in EPS of both AeS and AnS exhibited a greater binding capacity for MS2 compared to humic substances, consistent with findings regarding the EPS adsorption of heavy metals, antibiotics, and organic pollutants.^{22,27–29}

The peak intensities of functional groups before and after MS2 adsorption by EPS fractions of AeS and AnS were characterized (Figure 4). Based on the changes in peak intensity before and after virus adsorption, the functional groups involved in the virus adsorption of AS fractions were analyzed to identify the substances contributing to virus adsorption in each fraction. The peak at 3428 cm⁻¹ was attributed to the O-H and N-H stretching vibrations of amines, while the band in the range of 3200–3500 cm⁻¹ was associated with the O-H bond in hydroxyl functional groups.^{30,31} The intensity of the peaks in the EPS of both AeS and AnS decreased following MS2 adsorption, indicating that the -OH groups also served as active binding sites for MS2 adsorption.^{32,33} The decrease in the intensity of the CH₂ asymmetric stretch of hydrocarbons and the C-O, C-O-C stretch from polysaccharides peaks in EPS indicates that the hydrocarbon and polysaccharide in AeS provide active sites for virus

adsorption, which differs from the conclusion that the functional group of protein in EPS was involved in ciprofloxacin adsorption.²⁸ Meanwhile, the AS from A2O separated the polysaccharide with high virus adsorption.³⁵ Unlike AeMBR, where the peak intensity at 3428 cm⁻¹ changed, the remaining peak intensities in AnMBR did not exhibit significant alterations after MS2 adsorption. This discrepancy may be attributed to the fact that microorganisms in AnMBR and AeMBR degrade through distinct pathways, resulting in different consumption or production of related microbial metabolites.^{1,15} Among the fluorescent substances of the both AnS and AeS in EPS, mainly protein-like substances provided the adsorption of the virus. Functional groups of polysaccharides in AeS participate in viral adsorption.

Conclusions

The average removal efficiency of AeMBR was higher than that of AnMBR. The virus concentration in AS of the AnMBR was greater than that in the AeMBR, which was consistent with the predictions made by the pseudo-second-order kinetic model. S-EPS was the primary contributor to virus adsorption in AeS, and TB-EPS played a significant role in virus adsorption in AnS. Among the fluorescent substances in EPS of the both AeS and AnS, protein-like substances were primarily responsible for virus adsorption. Additionally, the functional groups of polysaccharides in AeS were involved in viral adsorption. The virus inactivation rate in the aerobic mixed liquor was higher than that in the anaerobic mixed liquor, which may explain the superior virus removal efficiency observed in the AeMBR compared to the AnMBR.

Limitations of the study

It is important to acknowledge that the synthetic sewage utilized in this study simulates actual sewage, with MS2 serving as a surrogate virus to investigate the virus removal efficiency in MBRs and the interactions between AS and viruses. However, the behavior of MS2 in synthetic sewage may not fully reflect the behavior of enteroviruses in real sewage environments. This discrepancy primarily arises from the fact the enteroviruses in actual sewage are typically particle-associated, whereas MS2 exists in a free state in synthetic sewage. Furthermore, as a non-enveloped virus, the mechanisms of the inactivation and adsorption of enveloped viruses in conjunction with AS differ significantly from those of enveloped viruses.

Table 2. Kinetic parameters of AS and their fractions for the adsorption of MS2 at 25°C

Parameter	K_2 (g/(PFU·min))	q_e (PFU/g)	R^2
AeS			
Untreated AeS	$3.06 \times 10^{(-11)}$	11.13 log ₁₀	0.998
After S-EPS extraction	$4.87 \times 10^{(-11)}$	10.23 log ₁₀	0.936
After LB-EPS extraction	$6.44 \times 10^{(-11)}$	10.29 log ₁₀	0.856
After TB-EPS extraction	–	–	–
AnS			
Untreated AnS	$7.078 \times 10^{(-11)}$	11.92 log ₁₀	0.999
After S-EPS extraction	$4.237 \times 10^{(-12)}$	11.19 log ₁₀	0.984
After LB-EPS extraction	$1.890 \times 10^{(-12)}$	11.04 log ₁₀	0.875
After TB-EPS extraction	–	–	–

Table 3. Variations in fluorescence intensities of EPS fractions

Fluorescence substances	S-EPS		B-EPS	
	Before adsorption	After adsorption	Before adsorption	After adsorption
AeS				
Marine humic acid	117	140	1312	1198
Tryptophan protein-like substance	205	113	1956	1736
Aromatic protein-like substance	–	–	227	230
AnS				
Tyrosine aromatic protein-like substance	626	398	1030	865
Tryptophan protein-like substance	208	259	1722	1598
Humic acid A	36	42	132	127
Humic acid B	42	57	104	91

RESOURCE AVAILABILITY

Lead contact

Further information and requests for resources and reagents should be directed to and will be fulfilled by the lead contact, Rong Chen (chenrong@xauat.edu.cn).

Materials availability

This study did not generate new unique reagents.

Data and code availability

- There is no dataset associated with this article.
- This article does not report the original code.
- Any additional information required to reanalyze the data reported in this article is available from the [lead contact](#) upon request.

ACKNOWLEDGMENTS

This work was supported by the National Science Found for Distinguished Young Scholars (No. 52325002), the International Science and Technology Cooperation Program of Shaanxi Province (No.2023-GHZD-27), and Science Foundation for Distinguished Young Scholars of Shaanxi Province (No.2022JC-31).

AUTHOR CONTRIBUTIONS

Conceptualization, J.F.Z. and R.C.; investigation, J.Z.; writing-original draft, J.F.Z.; writing-review and editing, R.C. and D.S.; visualization, J.F.Z. and J.Z.; supervision, R.C.; funding acquisition, R.C.

DECLARATION OF INTERESTS

The authors declare no competing interests.

STAR★METHODS

Detailed methods are provided in the online version of this paper and include the following:

- [KEY RESOURCES TABLE](#)
- [EXPERIMENTAL MODEL AND STUDY PARTICIPANT DETAILS](#)
- [METHOD DETAILS](#)
 - Membrane bioreactors and operating conditions
 - MS2 stock preparation and counting
 - Adsorbability experiment
 - Survivability experiment
 - Virus removal and recovery efficiency
 - EPS extraction and detection
 - Spectral analysis
 - Other analytical methods
 - Materials
- [QUANTIFICATION AND STATISTICAL ANALYSIS](#)
- [ADDITIONAL RESOURCES](#)

SUPPLEMENTAL INFORMATION

Supplemental information can be found online at <https://doi.org/10.1016/j.isci.2024.111450>.

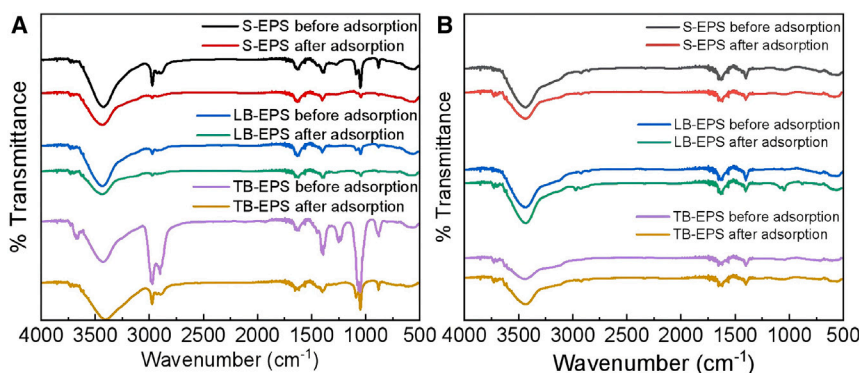


Figure 4. FTIR spectra of EPS fractions before and after MS2 adsorption

(A) AeS.
(B) AnS.

Received: July 30, 2024
Revised: September 10, 2024
Accepted: November 19, 2024
Published: November 22, 2024

REFERENCES

- Wang, K.M., Garcia, N.M., Soares, A., Jefferson, B., and McAdam, E.J. (2018). Comparison of fouling between aerobic and anaerobic MBR treating municipal wastewater. *H2Open J.* 1, 131–159. <https://doi.org/10.2166/h2oj.2018.109>.
- Xu, X., Dao, H., Bair, R., Uman, A.E., Yeh, D., and Zhang, Q. (2020). Discharge or reuse? Comparative sustainability assessment of anaerobic and aerobic membrane bioreactors. *J. Environ. Qual.* 49, 545–556. <https://doi.org/10.1002/jeq2.20012>.
- Prado, T., Silva, D.M., Guilayn, W.C., Rose, T.L., Gaspar, A.M.C., and Miagostovich, M.P. (2011). Quantification and molecular characterization of enteric viruses detected in effluents from two hospital wastewater treatment plants. *Water Res.* 45, 1287–1297. <https://doi.org/10.1016/j.watres.2010.10.012>.
- Prado, T., Fumian, T.M., Mannarino, C.F., Resende, P.C., Motta, F.C., Ep-pinghaus, A.L.F., Chagas do Vale, V.H., Braz, R.M.S., de Andrade, J.d.S.R., Maranhão, A.G., and Miagostovich, M.P. (2021). Wastewater-based epidemiology as a useful tool to track SARS-CoV-2 and support public health policies at municipal level in Brazil. *Water Res.* 191, 116810. <https://doi.org/10.1016/j.watres.2021.116810>.
- Zhang, J., Wu, B., Zhang, J., Zhai, X., Liu, Z., Yang, Q., Liu, H., Hou, Z., Sano, D., and Chen, R. (2022). Virus removal during sewage treatment by anaerobic membrane bioreactor (AnMBR): The role of membrane fouling. *Water Res.* 211, 118055. <https://doi.org/10.1016/j.watres.2022.118055>.
- Wu, B., Liu, H., Liu, Z., Zhang, J., Zhai, X., Zhu, Y., Sano, D., Wang, X., and Chen, R. (2022). Interface behavior and removal mechanisms of human pathogenic viruses in anaerobic membrane bioreactor (AnMBR). *Water Res.* 219, 118596. <https://doi.org/10.1016/j.watres.2022.118596>.
- Chaudhry, R.M., Nelson, K.L., and Drewes, J.E. (2015). Mechanisms of pathogenic virus removal in a full-scale membrane bioreactor. *Environ. Sci. Technol.* 49, 2815–2822. <https://doi.org/10.1021/es505332n>.
- Yang, W., Cai, C., and Dai, X. (2022). Interactions between virus surrogates and sewage sludge vary by viral analyte: Recovery, persistence, and sorption. *Water Res.* 210, 117995. <https://doi.org/10.1016/j.watres.2021.117995>.
- Chaudhry, R.M., Holloway, R.W., Cath, T.Y., and Nelson, K.L. (2015). Impact of virus surface characteristics on removal mechanisms within membrane bioreactors. *Water Res.* 84, 144–152. <https://doi.org/10.1016/j.watres.2015.07.020>.
- Yu, H.Q. (2020). Molecular insights into extracellular polymeric substances in activated sludge. *Environ. Sci. Technol.* 54, 7742–7750. <https://doi.org/10.1021/acs.est.0c00850>.
- Huang, L., Jin, Y., Zhou, D., Liu, L., Huang, S., Zhao, Y., and Chen, Y. (2022). A review of the role of extracellular polymeric substances (EPS) in wastewater treatment systems. *Int. J. Environ. Res. Public Health* 19, 12191. <https://doi.org/10.3390/ijerph191912191>.
- Liu, W., Song, X., Huda, N., Xie, M., Li, G., and Luo, W. (2020). Comparison between aerobic and anaerobic membrane bioreactors for trace organic contaminant removal in wastewater treatment. *Environ. Technol. Innov.* 17, 100564. <https://doi.org/10.1016/j.eti.2019.100564>.
- Ho, J., Stange, C., Suhrborg, R., Wurzbacher, C., Drewes, J.E., and Tiehm, A. (2022). SARS-CoV-2 wastewater surveillance in Germany: Long-term RT-digital droplet PCR monitoring, suitability of primer/probe combinations and biomarker stability. *Water Res.* 210, 1117977. <https://doi.org/10.1016/j.watres.2021.1117977>.
- Pinon, A., and Viallette, M. (2018). Survival of viruses in water. *Intervirology* 61, 214–222. <https://doi.org/10.1159/000484899>.
- Yao, Y., Xu, R., Zhou, Z., and Meng, F. (2021). Linking dynamics in morphology, components, and microbial communities of biocakes to fouling evolution: A comparative study of anaerobic and aerobic membrane bioreactors. *Chem. Eng. J.* 413, 127483. <https://doi.org/10.1016/j.cej.2020.127483>.
- Hamza, I.A., Jurzik, L., Stang, A., Sure, K., Uberla, K., and Wilhelm, M. (2009). Detection of human viruses in rivers of a densely-populated area in Germany using a virus adsorption elution method optimized for PCR analyses. *Water Res.* 43, 2657–2668. <https://doi.org/10.1016/j.watres.2009.03.020>.
- Barrios-Hernández, M.L., Pronk, M., Garcia, H., Boersma, A., Brdjanovic, D., van Loosdrecht, M.C.M., and Hooijmans, C.M. (2020). Removal of bacterial and viral indicator organisms in full-scale aerobic granular sludge and conventional activated sludge systems. *Water Res.* X 6, 100040. <https://doi.org/10.1016/j.wroa.2019.100040>.
- Ye, Y., Ellenberg, R.M., Graham, K.E., and Wigginton, K.R. (2016). Survivability, partitioning, and recovery of enveloped viruses in untreated municipal wastewater. *Environ. Sci. Technol.* 50, 5077–5085. <https://doi.org/10.1021/acs.est.6b00876>.
- Al-hazmi, H.E., Shokrani, H., Shokrani, A., Jabbour, K., Abida, O., Mousavi Khadem, S.S., Habibzadeh, S., Sonawane, S.H., Saeb, M.R., Bonilla-Petriciolet, A., and Badawi, M. (2022). Recent advances in aqueous virus removal technologies. *Chemosphere* 305, 135441. <https://doi.org/10.1016/j.chemosphere.2022.135441>.
- Chen, M., Lei, Q., Ren, L., Li, J., Li, X., and Wang, Z. (2021). Efficacy of electrochemical membrane bioreactor for virus removal from wastewater: Performance and mechanisms. *Bioresour. Technol.* 330, 124946. <https://doi.org/10.1016/j.biortech.2021.124946>.
- Armanious, A., Aeppli, M., Jacak, R., Refardt, D., Sigstam, T., Kohn, T., and Sander, M. (2016). Viruses at solid-water interfaces: A systematic assessment of interactions driving adsorption. *Environ. Sci. Technol.* 50, 732–743. <https://doi.org/10.1021/acs.est.5b04644>.
- Wei, D., Wang, B., Ngo, H.H., Guo, W., Han, F., Wang, X., Du, B., and Wei, Q. (2015). Role of extracellular polymeric substances in biosorption of dye wastewater using aerobic granular sludge. *Bioresour. Technol.* 185, 14–20. <https://doi.org/10.1016/j.biortech.2015.02.084>.
- Gordon, C., and Toze, S. (2003). Influence of groundwater characteristics on the survival of enteric viruses. *J. Appl. Microbiol.* 95, 536–544. <https://doi.org/10.1046/j.1365-2672.2003.02010.x>.
- Brackley, C.A., Lips, A., Morozov, A., Poon, W.C.K., and Marenduzzo, D. (2021). Mechanisms for destabilisation of RNA viruses at air-water and liquid-liquid interfaces. *Nat. Commun.* 12, 6812. <https://doi.org/10.1038/s41467-021-27052-7>.
- Barrios-hernández, M.L., Bettinelli, C., Mora-cabrera, K., Vanegas-camero, M., Garcia, H., Vossenberg, J.V.D., Prats, D., Brdjanovic, D., van Loosdrecht, M.C.M., and Hooijmans, C.M. (2021). Unravelling the removal mechanisms of bacterial and viral surrogates in aerobic granular sludge systems. *Water Res.* 195, 116992. <https://doi.org/10.1016/j.watres.2021.116992>.
- Garcia-Ochoa, F., and Gomez, E. (2009). Bioreactor scale-up and oxygen transfer rate in microbial processes: An overview. *Biotechnol. Adv.* 27, 153–176. <https://doi.org/10.1016/j.biotechadv.2008.10.006>.
- Wei, L., Li, Y., Noguera, D.R., Zhao, N., Song, Y., Ding, J., Zhao, Q., and Cui, F. (2017). Adsorption of Cu²⁺ and Zn²⁺ by extracellular polymeric substances (EPS) in different sludges: Effect of EPS fractional polarity on binding mechanism. *J. Hazard Mater.* 321, 473–483. <https://doi.org/10.1016/j.jhazmat.2016.05.016>.
- Zhang, H., Jia, Y., Khanal, S.K., Lu, H., Fang, H., and Zhao, Q. (2018). Understanding the role of extracellular polymeric substances on ciprofloxacin adsorption in aerobic sludge, anaerobic sludge, and sulfate-reducing bacteria sludge systems. *Environ. Sci. Technol.* 52, 6476–6486. <https://doi.org/10.1021/acs.est.8b00568>.
- Pan, X., Liu, J., Zhang, D., Chen, X., Song, W., and Wu, F. (2010). Binding of dicamba to soluble and bound extracellular polymeric substances (EPS)

- from aerobic activated sludge: A fluorescence quenching study. *J. Colloid Interface Sci.* **345**, 442–447. <https://doi.org/10.1016/j.jcis.2010.02.011>.
30. Chergui, A., Kerbachi, R., and Junter, G.A. (2009). Biosorption of hexacyanoferrate(III) complex anion to dead biomass of the basidiomycete *pleurotus mutilus*: Biosorbent characterization and batch experiments. *Chem. Eng. J.* **147**, 150–160. <https://doi.org/10.1016/j.cej.2008.06.029>.
 31. Jain, R., Jordan, N., Weiss, S., Foerstendorf, H., Heim, K., Kacker, R., Hübner, R., Kramer, H., Van Hullebusch, E.D., Farges, F., and Lens, P.N.L. (2015). Extracellular polymeric substances govern the surface charge of biogenic elemental selenium nanoparticles. *Environ. Sci. Technol.* **49**, 1713–1720. <https://doi.org/10.1021/es5043063>.
 32. Chan, K.Y., Xu, L.C., and Fang, H.H.P. (2002). Anaerobic electrochemical corrosion of mild steel in the presence of extracellular polymeric substances produced by a culture enriched in sulfate-reducing bacteria. *Environ. Sci. Technol.* **36**, 1720–1727. <https://doi.org/10.1021/es011187c>.
 33. Meng, F., Zhang, H., Yang, F., and Liu, L. (2007). Characterization of cake layer in submerged membrane bioreactor. *Environ. Sci. Technol.* **41**, 4065–4070. <https://doi.org/10.1021/es062208b>.
 34. Jia, F., Yang, Q., Liu, X., Li, X., Li, B., Zhang, L., and Peng, Y. (2017). Stratification of extracellular polymeric substances (EPS) for aggregated anammox microorganisms. *Environ. Sci. Technol.* **51**, 3260–3268. <https://doi.org/10.1021/acs.est.6b05761>.
 35. Miura, T., Sano, D., Suenaga, A., Yoshimura, T., Fuzawa, M., Nakagomi, T., Nakagomi, O., and Okabe, S. (2013). Histo-blood group antigen-like substances of human enteric bacteria as specific adsorbents for human noroviruses. *J. Virol.* **87**, 9441–9451. <https://doi.org/10.1128/jvi.01060-13>.
 36. You, G., Wang, P., Hou, J., Wang, C., Xu, Y., Miao, L., Lv, B., Yang, Y., and Liu, Z. (2017). Insights into the short-term effects of CeO₂ nanoparticles on sludge dewatering and related mechanism. *Water Res.* **118**, 93–103. <https://doi.org/10.1016/j.watres.2017.04.011>.
 37. Baird, R.B., Eaton, A.D., and Rice, E.W. (2017). *Standard Methods for the Examination of Water and Wastewater, 23rd Edition* (American Public Health Association, American Water Works Association, Water Environment Federation).

STAR★METHODS

KEY RESOURCES TABLE

REAGENT or RESOURCE	SOURCE	IDENTIFIER
Bacterial and virus strains		
MS2	ATCC	ATCC 15597-B1
<i>E.coli</i>	ATCC	ATCC 155977

EXPERIMENTAL MODEL AND STUDY PARTICIPANT DETAILS

No experimental models were used in this study.

METHOD DETAILS

Membrane bioreactors and operating conditions

AeMBR and AnMBR were operated under identical conditions to treat synthetic sewage spiked with MS2 bacteriophage, utilizing a polyvinylidene fluoride (PVDF) flat membrane with a membrane pore of 0.2 μm (Figure S10). The synthetic sewage contained a chemical oxygen demand (COD) of 500 mg/L and essential nutrients for microbial growth, with detailed composition provided in Table S1. MS2 stock was introduced daily into the synthetic sewage, achieving a final concentration of approximately 10^{10} PFU/L. The substrate tank was maintained at 4°C to prevent the COD degradation and MS2 inactivation. The seed sludge for AeMBR was sourced from the aerobic tank of a local sewage treatment plant in Xi'an, China, while seed sludge of AnMBR was obtained from an AnMBR that had been operating stably for over two years in our laboratory. During operation, the mixed liquor suspended solid (MLSS) concentration of the MBRs was maintained at 10 g/L. The sludge retention time (SRT) for AeMBR and AnMBR was calculated as approximately 65 days and 238 days, respectively. Control of membrane fouling and ensure mixing of the bulk sludge by aeration from the bottom of the MBR at a rate of 4.5 L/min, and the gas of AnMBR and AeMBR originated from the biogas produced by anaerobic digestion and air, respectively. The dissolved oxygen (DO) concentration in the mixed liquor of AeMBR was kept at approximately 2 mg/L. A digital pressure meter (Sinomeasure; China) was installed between the membrane module and the effluent pump to record the transmembrane pressure (TMP). Other operating conditions for MBRs were performed as previously described.⁵ Additionally, a separate group of AeMBR and AnMBR was operated under same operating parameters to treat synthetic sewage without MS2, in order to obtain AS for conducting adsorbability experiment, survivability experiment and spectral analyses. Although different batches of AS were utilized for the adsorbability experiments, survivability experiments and spectral analyses, each experiment employed a consistent batch of AS within its respective procedure.

MS2 stock preparation and counting

The preparation of bacteriophage MS2 (ATCC 15597-B1) stock and the MS2 counting method were conducted as described by Zhang et al.⁵ The concentration of MS2 in the mixed liquor was assessed by separately measuring the liquid and solid phases. Initially, the liquid and solid phases were isolated by centrifugation at 4°C for 60 min at 10,000 g (theoretical size cutoff 340 nm). The supernatant was carefully collected to determine the volume and MS2 concentration, allowing for the quantification MS2 associated with the liquid phase. The solid phase was then resuspended in a 10% tris-glycine beef extract buffer, matching the volume of the mixed liquor, and mixed thoroughly. After thorough mixing, the sample was incubated in isothermal shaker at 25°C with shaking at 100 rpm for 30 min to elute MS2 from solid phase, followed by centrifugation at 10,000 g for another 30 min. The eluent was carefully collected to measure the MS2 concentration, thus determining the MS2 associated with the solid phase. The overall MS2 concentration in the mixed liquor was calculated using the following equation:

$$C_{mix} = \frac{C_l V_l + \frac{C_e V_e}{R\%}}{V_{mix}} \quad (\text{Equation 1})$$

where C_l (PFU/L) and V_l (L) are the MS2 concentration and the volume of the liquid phase, respectively. C_e (PFU/L) and V_e (L) are the MS2 concentration and the volume of eluent, respectively. C_{mix} (PFU/L) and V_{mix} (L) are the MS2 concentration and the volume of mixed liquor, respectively. $R\%$ is the viral recovery efficiency from AS.

Adsorbability experiment

The MLSS concentration in MBRs was generally maintained between 6 g/L and 10 g/L. Consequently, the adsorption kinetics of the AS at concentrations between 6 g/L and 10 g/L were investigated by a series of batch tests. The MS2 stock was spiked into mixed liquor, which was then stirred and incubated at 25°C, 120 rpm. Regular samples were taken to determine the MS2 concentration in the liquid phase. The adsorption efficiency and the amount of MS2 adsorbed q_t (PUF/g) was calculated using the following equation:

$$\text{Removal efficiency (\%)} = \frac{C_0 - C_t}{C_0} \quad (\text{Equation 2})$$

$$q_t = \frac{(C_0 - C_t) \times V}{m} \quad (\text{Equation 3})$$

where C_t (PFU/L) is the concentration of adsorbate at time t (min), V (L) is the volume of adsorbate solution, m (g) is the mass of AS, q_t (PFU/g) is the amount adsorbed at time t (min).

In order to better understand the mechanism and rate-control step in the overall adsorption process, the adsorption kinetics data for MS2 were evaluated using the pseudo-second-order model. The pseudo-second-order equation model is expressed as following:

$$\frac{t}{q_t} = \frac{1}{k_2 q_e^2} + \frac{1}{q_e} t \quad (\text{Equation 4})$$

where q_t (PFU/g) is the amount adsorbed at time t , q_e (PFU/g) is the amount adsorbed at equilibrium, k_2 (PFU/(g min)) is the equilibrium rate constant of the pseudo-second-order kinetic model.

Survivability experiment

AeS and AnS were collected from the AeMBR and AnMBR that treated MS2-free sewage, respectively, and placed in serum bottles. Headspace of serum bottle containing AnS was purged with nitrogen gas for 2 min to remove oxygen, and then seal with a butyl rubber stopper. The serum bottle containing AeS was left unsealed to allow for oxygen supply, maintaining a DO concentration of about 2 mg/L. MS2 stock was spiked into serum bottles, achieving a final concentration of 10^{10} PFU/L. The AS with spiked MS2 were promptly stirred and incubated at 25°C. During the incubation period, regular samples were taken to measure the MS2 concentration in the mixed liquor. Simultaneously, the AS was inactivated at high temperature to investigate the MS2 inactivation rate in both inactivated AeS and AnS. The specific procedure for high-temperature inactivation of AS involved autoclaving at 121°C for 15 min. Additionally, the survival of virus in AeS was studied at DO concentrations of 0 mg/L, 2 mg/L, 4 mg/L, respectively. All samples were analyzed in triplicate. The inactivation kinetics of virus surrogate was fitted to virus inactivation kinetics using the following equation:

$$\ln \frac{C_t}{C_0} = -K_{obs} t \quad (\text{Equation 5})$$

where C_0 (PFU/L) and C_t (PFU/L) represent the concentrations of MS2 at time 0 and t , respectively, and K_{obs} is the virus inactivation kinetics constant (day^{-1}).

Virus removal and recovery efficiency

The experiments to determine the recovery efficiency of MS2 from AS were performed as follows: mixed liquor sample was introduced into the serum bottles, which were then sealed with butyl rubber stoppers. MS2 stock identified the virus amount was spiked into the serum bottles, and the serum bottles were mixed to ensure MS2 was adsorbed onto AS. Subsequently, a quantitative aliquot of mixed liquor was transferred from the serum bottles to centrifuge tubes to determine liquid-phase and solid-phase associated MS2, respectively. It was hypothesized that no inactivation occurred during the process. The recovery efficiency of MS2 was calculated by the formulae:

$$\text{MS2 recovery efficiency (\%)} = \frac{C_e V_e}{S_{spiked} - C_i V_i} \quad (\text{Equation 6})$$

where C_i (PFU/L) and V_i (L) are the MS2 concentration and the volume of liquid phase, respectively. C_e (PFU/L) and V_e (L) are the MS2 concentration and the volume of eluent, respectively. S_{spiked} (PFU) represents the total amount of MS2 spiked. The MS2 recovery efficiency from AeS, AnS, inactivated AeS, and inactivated AnS is 23.96%, 8.07%, 7.33%, 5.21%, respectively.

MS2 removal efficiency could be expressed as LRV and was calculated using Equation 7. LRV_{MBR} and LRV_M were applied to represent the overall removal and membrane rejection, respectively. Influent and effluent samples of MBRs were collected every 2 days or 3 days and then filtered by a 0.22 μm membrane filter for infection assay to obtain the virus removal efficiency by MBRs. The virus concentration in the mixed liquor was measured regularly to calculate the virus rejection efficiency of the membrane.

$$LRV = -\log \frac{C_e}{C_i} \quad (\text{Equation 7})$$

where C_i (PFU/L) and C_e (PFU/L) represent the MS2 concentrations before and after treatment, respectively.

EPS extraction and detection

EPS were extracted from AS using a combination of centrifugation and a cation exchange resin extraction method.³⁶ Briefly, a 40 mL AS sample was centrifuged at 4,000 rpm for 10 min at 4°C. The resulting supernatant was filtered through a 0.45 µm filter to obtain the S-EPS. The remaining sediment was re-suspended with a 5‰ NaCl solution. Afterward, cation exchange resin (DOWEX R Marathon C, Na⁺ form, Sigma-Aldrich, USA) was then added at a ratio of 60 g per gram of MLVSS, and mixed thoroughly. The mixture was centrifuged for 10 min at 10,000 rpm, at 4°C, and the supernatant was filtered through a 0.45 µm filter to obtain the LB-EPS. The remaining sediment was re-suspended in a 5‰ NaCl solution, and shaken at 200 rpm, at 25°C for 4 h. Following, it was centrifuged again at 10,000 rpm for 10 min at 4°C, and the supernatant was decanted and filtered through a 0.45 µm membrane to obtain TB-EPS. The carbohydrate content in EPS was quantified using H₂SO₄/phenol oxidation and a colorimeter method, and the protein content was determined using the Folin-Ciocalteu methods. All analyses were conducted in duplicate.

Spectral analysis

The three-dimensional excitation-emission matrix (3D-EEM) fluorescence spectra of EPS fractions before and after MS2 adsorption were obtained for a three-dimensional fluorescence spectrophotometer (F-7000; Hitachi, Japan). The excitation wavelength domain was set from 250 nm to 550 nm, and the emission range was from 200 nm to 400 nm. The slit widths for both excitation and emission monochromator were set at 5 nm, and the scan speed was 12000 nm/min. 3D-EEM of each sample underwent spectral subtraction with a deionized water blank to eliminate Rayleigh and Raman scattering and other background noises. Parallel factor analysis (PARAFAC) was employed to analyze the fluorescence intensity of EPS fractions before and after MS2 adsorption. Additionally, the functional groups of EPS fractions before and after MS2 adsorption was identified using Fourier transform infrared spectroscopy (FTIR) (IS50, Nicolet, American) with wave number in the range of 4000 cm⁻¹ to 400 cm⁻¹.

Other analytical methods

The COD concentration of influent and effluent, MLSS and MLVSS concentration in MBRs were determined as per the Standard Methods.³⁷ The DO concentration was measured by a HACH HQ30d corresponding probe (LDO101, HACH Company, USA). The methane (CH₄) content of the biogas was measured with a gas chromatograph (GC-7900; Tianmei, China) equipped with a thermal conductivity detector. A laser granularity distribution analyzer (LS 230/SVM+; Beckmen Coulter, USA) was used to analyze the particle distribution of mixed liquor. The zeta potential of mixed liquor was measured by electrophoretic light scattering method (Malvern Zetasizer Nano-ZS90).

Materials

The purity of all chemical agents is analytical grade at least and use without further purification. 10% tris-glycine beef extract buffer (10% tris-glycine, CAS556-33-2, Yeast extract), nutrient agar (CM107) was purchased from Beijing Land Bridge Co., Ltd (Beijing, China), tryptone (CM001) was purchased from Beijing Land Bridge Co., Ltd (Beijing, China), Luria-Bertani agar (CM158) was purchased from Beijing Land Bridge Co., Ltd (Beijing, China), agar powder (01-023) was purchased from AOBX Co., Ltd (Beijing, China), Yeast extract was purchased from AOBX Co., Ltd (Beijing, China), Na ion cation exchange resin (CAS: 150604-77-6) was purchased from Merck KGaA Darmstadt (Germany), 0.45 µm mixed cellulose ester membrane and 0.22 µm mixed cellulose ester membrane were purchased from Shanghai Xin Ya Purification Equipment Co., Ltd (Beijing, China), 4% BSA solution (CAS: 9048-46-8) was purchased from Merck KGaA Darmstadt (Germany), Folin & Ciocalteus phenol reagent (Cat.No.F8060) was purchased from Solarbio science & technology Co., Ltd (Beijing, China), Phosphate-buffered saline (G0002-2L) was purchased from Huhan Service-bio Co., Ltd (Huhan, China).

QUANTIFICATION AND STATISTICAL ANALYSIS

All data are presented as means ± the standard deviations (s.d.) from a minimum of three independent experiments. Origin 2022 was used to produce all bar chart figures.

ADDITIONAL RESOURCES

There no additional resources.